information services
gwasanaethau gwybodaeth

New Insights into the Activation and Deactivation of Au/CeZrO₄ in the Low-Temperature Water-Gas Shift Reaction

James H. Carter,[a] Xi Liu,[b] Qian He,[a] Sultan Althahban,[c] Ewa Nowicka,[a] Simon J. Freakley,[a] Liwei Niu,[b] David J. Morgan,[a] Yongwang Li,[b] J. W. (Hans) Niemantsverdriet,[b,d] Stanislaw Golunski,[a] Christopher J. Kiely[a,c] and Graham J. Hutchings*[a]

[a]Cardiff Catalysis Institute, School of Chemistry, Cardiff University, Main Building, Park Place, Cardiff, CF10 3AT, UK.

[b]SynCat@Beijing, Synfuels China Technology Co., Ltd, Beijing, 101407, China

[c]Department of Materials Science and Engineering, Lehigh University, 5 East Packer Avenue, Bethlehem, PA 18015-3195, USA.

[d]SynCat@DIFFER, Syngaschem BV, PO Box 6336, 5600 HH, Eindhoven, The Netherlands

*Correspondence to Graham J. Hutchings

Tel: +44 29 2087 4059, Fax: (+44) 2920-874-030, E-mail: hutch@cardiff.ac.uk

Abstract:

Gold on ceria-zirconia is one of the most active catalysts for the low-temperature water-gas shift reaction (LTS), a key stage of upgrading H_2 reformate streams for fuel cells. However, this catalyst rapidly deactivates on-stream and the mechanism remains unclear. Using stop-start scanning transmission electron microscopy (STEM) to follow *the exact same area of the sample* at different stages of the LTS reaction, as well as complementary X-ray photoelectron spectroscopy, we observed the activation and deactivation of the catalyst at various stages. During the heating of the catalyst to reaction temperature, we observed the formation of small Au nanoparticles (1-2 nm) from sub-nm Au species. These nanoparticles were then seen to agglomerate further over 48 h on-stream, most rapidly in the first 5 h when the highest rate of deactivation was observed. These findings suggest that the primary deactivation process consists of the loss of active sites through the agglomeration and possible dewetting of Au nanoparticles.

Supported gold nanoparticles are remarkably active catalysts for a range of reactions including carbon monoxide oxidation[1] and the low-temperature water-gas shift reaction (LTS).[2, 3] The latter reaction has gained a renewed interest in the context of proton exchange membrane (PEM) fuel cells[3, 4] as the LTS reaction can be used to purify reformate streams, often containing percent levels of CO. As the reaction is equilibrium-limited at high temperatures, highly active LTS catalysts are needed to ensure their efficient operation. $Au/CeZrO_4$ was identified as a candidate for this application, exhibiting remarkably high conversions at low temperatures.[3] However, this catalyst rapidly deactivates under reaction conditions.

Goguet *et al.* published the most complete activation-deactivation model for $Au/CeZrO_4$, using *in situ* X-ray photoelectron spectroscopy (XPS), *in situ* diffuse-reflectance infrared Fourier Transform spectroscopy (DRIFTS) and density functional theory (DFT).[5] They proposed that the catalyst was activated under reaction conditions, when ionic gold species were reduced to form discrete metallic nanoparticles that interacted strongly with the support. However, the activity decreased with time-on-line, as the gold de-wetted from the support by changing shape from hemi-spherical to spherical nanoparticles. This significantly reduced the physical extent of the metal-support interface – the proposed active center. However, this de-wetting process has not been directly demonstrated experimentally. In an earlier study, *in situ* extended X-ray absorption fine structure (EXAFS) was used to rule out particle sintering on $Au/CeZrO_4$ as a relevant deactivation process[3] although this was shown to be the primary cause of deactivation in Au/CeO_2 and Pr-doped CeO_2.[6] Significantly, electron microscopy has not yet been implemented to help explain the processes that drive the deactivation of $Au/CeZrO_4$, possibly due to the poor mass contrast between Au and Ce that limits the visibility of very small Au species. The formation of surface carbonates as a

cause of deactivation on Au/CeO_2 was reported[7] but was disregarded for $Au/CeZrO_4$.[5] High angle annular dark field scanning transmission electron microscopy (HAADF-STEM) analysis of Au/CeO_2, revealed evidence of particle sintering as well as a change in Au morphology after exposure to CO and H_2O at 290 °C.[8] However, the gas composition did not include CO_2 or H_2, which are important contributors in the deactivation rate.[5, 9]

Here we focus on the evolution of Au species throughout the lifetime of 2 wt% $Au/CeZrO_4$. 'Stop-start' HAADF-STEM, *ex situ* HAADF-STEM and XPS were utilized to evaluate the changes that occur during the LTS reaction. The stop-start strategy allows the observation of *exactly the same* area of sample after exposure to reaction conditions. A detailed description of the methodology is provided in the Supporting Information. Fig. 1 shows the intervals when the catalyst was characterized, which include the fresh catalyst, after it was heated to reaction temperature in N_2 and after various times on-stream. The initial activity of 1.35 mM CO h^{-1} dropped by 26% after 5 h on-stream, and a further 24% over the next 43 h. Complementary XRD analysis, carried out to verify if structural changes to the support had occurred (or if reflections due to Au could be measured), showed only reflections due to the $CeZrO_4$ support, which remained unchanged after 48 h on-stream (Fig. S1).

A detailed analysis of the microstructure of the $CeZrO_4$ (Solvay) support is presented in Figs. S2 and S3. When fresh samples of the 2 wt% $Au/CeZrO_4$ catalyst were compared with samples after 48 h on-stream using HAADF-STEM and BF-TEM (Figs. 2 and S4), 5-10 nm Au particles were found in both, whereas additional particles in the 1-2 nm size range were mostly detected in the used catalyst. Furthermore, X-ray energy-dispersive spectroscopy (XEDS) analysis detected the presence of Au decorating the support where no particles were visible, implying the presence of unresolved sub-nm clusters or atomically-dispersed Au on the $CeZrO_4$ surface. The difficulties in visualizing atomically-dispersed Au on CeO_2 using

4

HAADF imaging have been described previously.[10, 11] Fig. S5 demonstrates that clearly distinguishing atomically-dispersed surface Au from substitutional Zr atoms in the $CeZrO_4$ support is even more challenging.

Fig. S6 shows some representative BF- and HAADF-STEM images of the larger (> 5 nm) Au nanoparticles in the fresh and 48 h used 2 wt% $Au/CeZrO_4$ catalyst. A common feature noted in the fresh catalyst was that the Au particles were often preferentially located in the three-fold intersection points or in the planar crevices between neighboring $CeZrO_4$ grains (Fig. S6a). Also apparent is the fact that the Au particles tend to exhibit distinct {111} and {200} type surface facets and seem to form planar interfaces with the mixed oxide support grains (Figs. S6 b) and c)). After 48 h on-stream, the Au nanoparticles appeared more rounded and prone to multiple twinning, with less interfacial contact than their unused counterparts (Figs. S6 d), e) and f)), which could indicate partial de-wetting from the support as previously proposed,[5] but could also be caused by the restructuring of particles as they sinter.

Fig. 3 shows stop-start HAADF-STEM images of the catalyst at four stages of the reaction: a) fresh; b) after the heat ramp in N_2; c) after 5 min on-stream and d) after 12 h on-stream. The reaction conditions are the same as those used to acquire the catalytic data in Fig. 1. The significance of the sample heated under N_2 is that it represents the sample just before the reaction is initiated. The cause of further changes to the catalyst sample after this point can therefore be attributed to the LTS reaction and are most likely deactivation processes. Examination of the sample after 5 min allows the most unstable species present in the heated catalyst to be identified. Finally, the sample after 12 h on-stream reveals the changes to the catalyst after longer term exposure to LTS conditions.

From Fig. 3, it is evident that small (~1 nm) gold nanoparticles form after heating to reaction temperature, which were not present in the fresh sample, as highlighted by the white

5

dashed line circle. This is consistent with the XEDS measurements in Fig. 2 that suggested the presence of un-resolvable sub-nm species such as clusters, oligomers and atomically-dispersed Au^{3+} in the fresh catalyst, which can agglomerate into detectable 1 nm particles during the initial temperature ramp in N_2. After 5 min on-stream, these smaller nanoparticles coalesce into an even larger nanoparticle *ca.* 5 nm in size (black arrows in Fig. 3c)), illustrating their tendency to sinter if in close spatial proximity. After 12 h on-stream this 5 nm nanoparticle is largely unchanged. Likewise, 10 nm scale Au particles (Fig. 3, inset a) – d)) remained stable throughout the reaction. The formation of 1-2 nm nanoparticles under the N_2 heating ramp was commonly observed throughout the samples analyzed and in some cases, if not in close proximity to other particles, exhibited good stability during the 12 h reaction (Fig. S7).

Additionally, 'stop-start' experiments revealed that Au nanoparticles already formed in the fresh catalyst can agglomerate and sinter under LTS conditions. Fig. 4 shows a nanoparticle initially 5 nm in diameter (dashed white circle), which after 12 h on-stream increases in size to ~10 nm. While the smaller (~1 nm) Au species appeared to sinter at a faster rate than the larger (~ 5 nm) nanoparticles, significantly more Au atoms are required for an increase of 5 nm to 10 nm, than for an increase of 1 nm to 4 nm. Therefore, relatively small changes in the size of the larger nanoparticles represent the loss of a large number of smaller Au species. Our experiments clearly show that rapid agglomeration of sub-nm Au species occurred while heating the catalyst to reaction temperature and under LTS conditions. Likewise, small highly dispersed Au nanoparticles, as well as larger nanoparticles, agglomerated further during the reaction, suggesting that the deactivation mechanism of the 2 wt% $Au/CeZrO_4$ catalyst is related to a loss of active sites through the agglomeration of ultra-small Au species.

Due to the inherently small sample size and qualitative nature of electron microscopy, additional characterization by XPS was carried out on a comparable set of samples that were exposed the same reaction conditions for similar times on-stream. The Au 4f region (Fig. S8) gives valuable information on the form of Au present in the catalyst and is comprised of three distinct species: namely Au^0 (84.0 eV) and Au^{3+} (86.1 eV), and a species at 85.0 eV. The assignment of the latter species, denoted Au^{0*}, remains controversial with some studies attributing it to small gold nanoparticles or clusters[12] whereas others relate it to positively charged gold species.[13] Our microscopy supports an assignment of the Au^{0*} species as small Au nanoparticles or clusters. Quantification of the fraction of each Au species present for each sample in this set is shown in Table 1. The fresh catalyst contains a high concentration of Au^{3+} and Au^{0*} indicating the presence of numerous small Au species including clusters, sub-nm species and atomically-dispersed Au. After the heat ramp under N_2, the Au^{3+} content of the sample decreased from 14.5% to 7.1% while the Au^{0*} content decreased from 18.4% to 15.0%. The loss of Au^{3+} is consistent with the agglomeration of sub-nm species such as atomically-dispersed Au cations into clusters and nanoscopic particles. Likewise, the loss of Au^{0*} can be accounted for by the agglomeration of clusters and small (1–2 nm) Au nanoparticles into larger nanoparticles. After 5 h on-stream, the time interval where the most rapid deactivation was measured, there was no significant Au^{3+} remaining in the sample, suggesting that all of the atomically-dispersed species had agglomerated into clusters and nanoparticles. Even though the Au^{0*} fraction did not significantly change over the 5 min to 5 h time period, these species were not necessarily stable throughout this time. It is likely that the Au^{3+} species lost during this time-period were replenishing the population of Au^{0*} species that were eventually absorbed into larger Au^0 nanoparticles. The strong correlation between the simultaneous loss of Au^{3+} and catalytic activity could indicate that the Au^{3+} species is

highly active but very unstable in this system. The ability of Au^{3+}, or atomically-dispersed Au, to catalyze the LTS reaction has received much attention in recent years[14] and developing synthetic methods of stabilizing such species is a subject of rigorous investigation.[15] From our study, it is probable that sub-nm Au clusters are also active and the rapid loss of activity noted could be partly due to clusters present at the start of the reaction that sinter into larger, less active nanoparticles, therefore it is not clear if the atomically-dispersed Au is catalyzing the LTS reaction. A recent study by Behm and co-workers on Au/CeO_2 showed that small metallic Au nanoparticles were predominantly responsible for the catalytic activity.[16] The fact that some catalytic activity remains after the complete loss of Au^{3+} indicates that a hierarchy of activity could exist whereby a multitude of different Au species are active, each having a different intrinsic activity. Such a hierarchy of activity was recently demonstrated for low-temperature CO oxidation over Au/Fe_2O_3[17] and Au/CeO_2.[10]

After 48 h on-stream, the $Au^{0}*$ concentration decreased slightly, indicating a slower rate of particle sintering, consistent with the testing data that showed that the rate of deactivation slowed after 5 h. It is likely that the most active species, in the form of sub-nm Au, are also the least stable and these are depleted after the first 5 h of the reaction, leaving larger, less active Au nanoparticles that continue to deactivate by sintering and possibly de-wetting from the support. The XPS analysis of the Au 4f region corroborated the findings from the stop-start STEM experiments, indicating the physical processes observed using such a small sample size were representative of the 'bulk' catalyst in a fixed-bed flow reactor.

In summary, electron microscopy and XPS investigations show that the deactivation of $Au/CeZrO_4$ in the LTS reaction proceeds primarily through gold agglomeration. Using stop-start STEM analysis, we were able to differentiate between the pre-reaction thermal agglomeration of sub-nm clusters and atomically dispersed Au species and the reaction-

8

induced sintering and de-wetting of nanoparticles that occurred during the LTS reaction. The most rapid agglomeration was of atomically-dispersed Au and sub-nm clusters undetectable by HAADF-STEM, into small (1-2 nm) Au nanoparticles which subsequently sintered into larger Au nanoparticles during the LTS reaction. Finally, there was also evidence of larger nanoparticles steadily sintering over the course of the reaction. These data provide strong evidence that particle agglomeration is a key deactivation process in the LTS reaction over 2 wt% $Au/CeZrO_4$ and that a hierarchy of active sites exists for this reaction. It also highlights the importance of synthesizing materials with strong metal-support interactions when developing stable Au-based catalysts for the LTS reaction.

References

[1] M. Haruta, T. Kobayashi, H. Sano, N. Yamada, *Chem. Lett.* **1987**, *16*, 405.

[2] Q. Fu, H. Saltsburg, M. Flytzani-Stephanopoulos, *Science* **2003**, *301*, 935.

[3] D. Tibiletti, A. Amieiro-Fonseca, R. Burch, Y. Chen, J. M. Fisher, A. Goguet, C. Hardacre, P. Hu, A. Thompsett, *J. Phys. Chem. B* **2005**, *109*, 22553.

[4] W. L. Deng, M. Flytzani-Stephanopoulos, *Angew. Chem. Int. Ed.* **2006**, *45*, 2285; W. Ruettinger, O. Ilinich, R. J. Farrauto, *J. Power Sources* **2003**, *118*, 61.

[5] A. Goguet, R. Burch, Y. Chen, C. Hardacre, P. Hu, R. W. Joyner, F. C. Meunier, B. S. Mun, A. Thompsett, D. Tibiletti, *J. Phys. Chem. C* **2007**, *111*, 16927.

[6] L. Ilieva, P. Petrova, I. Ivanov, G. Munteanu, M. Boutonnet, J. W. Sobczac, W. Lisowski, Z. Kaszkur, P. Markov, A. M. Venezia, T. Tabakova, *Mater. Chem. Phys.* **2015**, *157*, 138.

[7] Y. Denkwitz, A. Karpenko, V. Plzak, R. Leppelt, B. Schumacher, R. J. Behm, *J. Catal.* **2007**, *246*, 74.

[8] Y. Lin, Z. Wu, J. Wen, K. Ding, X. Yang, K. R. Poeppelmeier, L. D. Marks, *Nano Lett.* **2015**, *15*, 5375.

[9] A. Luengnaruemitchai, S. Osuwan, E. Gulari, *Catal. Comm.* **2003**, *4*, 215.

[10] L. W. Guo, P. P. Du, X. P. Fu, C. Ma, J. Zeng, R. Si, Y. Y. Huang, C. J. Jia, Y. W. Zhang, C. H. Yan, *Nat. Comm.* **2016**, *7*, 13481, doi: 10.1038/ncomms13481.

[11] C. E. Stere, J. A. Anderson, S. Chansai, J. J. Delgado, A. Goguet, W. G. Graham, C. Hardacre, S. F. R. Taylor, X. Tu, Z. Y. Wang, H. Yang, *Angew. Chem. Int. Ed.* **2017**, *56*, 5579.

[12] D. Dalacu, J. E. Klernberg-Sapieha, L. Martinu, *Surf. Sci.* **2001**, *472*, 33; E. A. Willneff, S. Braun, D. Rosenthal, H. Bluhm, M. Havecker, E. Kleimenov, A. Knop-Gericke, R. Schlogl, S. L. M. Schroeder, *J. Am. Chem. Soc.* **2006**, *128*, 12052; P. Rodriguez, D. Plana, D. J. Fermin, M. T. M. Koper, *J. Catal.* **2014**, *311*, 182; K. Luo, D. Y. Kim, D. W. Goodman, *J. Mol. Catal. A Chem.* **2001**, *167*, 191; J. H. Carter, S. Althahban, E. Nowicka, S. J. Freakley, D. J. Morgan, P. M. Shah, S. Golunski, C. J. Kiely, G. J. Hutchings, *ACS Catal.* **2016**, *6*, 6623.

[13] D. Boyd, S. Golunski, G. R. Hearne, T. Magadzu, K. Mallick, M. C. Raphulu, A. Venugopal, M. S. Scurrell, *App. Catal. A Gen.* **2005**, *292*, 76.

[14] M. Flytzani-Stephanopoulos, *Acc. Chem. Res.* **2014**, *47*, 783-792.

[15] M. Flytzani-Stephanopoulos, B. C. Gates, *Annu. Rev. Chem. Biomol.* **2012**, *3*, 545.

[16] A. M. Abdel-Mageed, G. Kučerová, J. Bansmann, J. R. Behm, *ACS Catal.* **2017**, *7*, 6471.

[17] Q. He, S. J. Freakley, J. K. Edwards, A. F. Carley, A. Y. Borisevich, Y. Mineo, M. Haruta, G. J. Hutchings, C. J. Kiely, *Nat. Comm.* **2016**, *7*, 12905, doi: 10.1038/ncomms12905.

Table 1. The evolution of Au oxidation states in the 2 wt% $Au/CeZrO_4$ catalyst, before, after N_2 pre-treatment and throughout the LTS reaction as monitored by *ex situ* XPS measurement and quantified using the Au 4f spectral region.

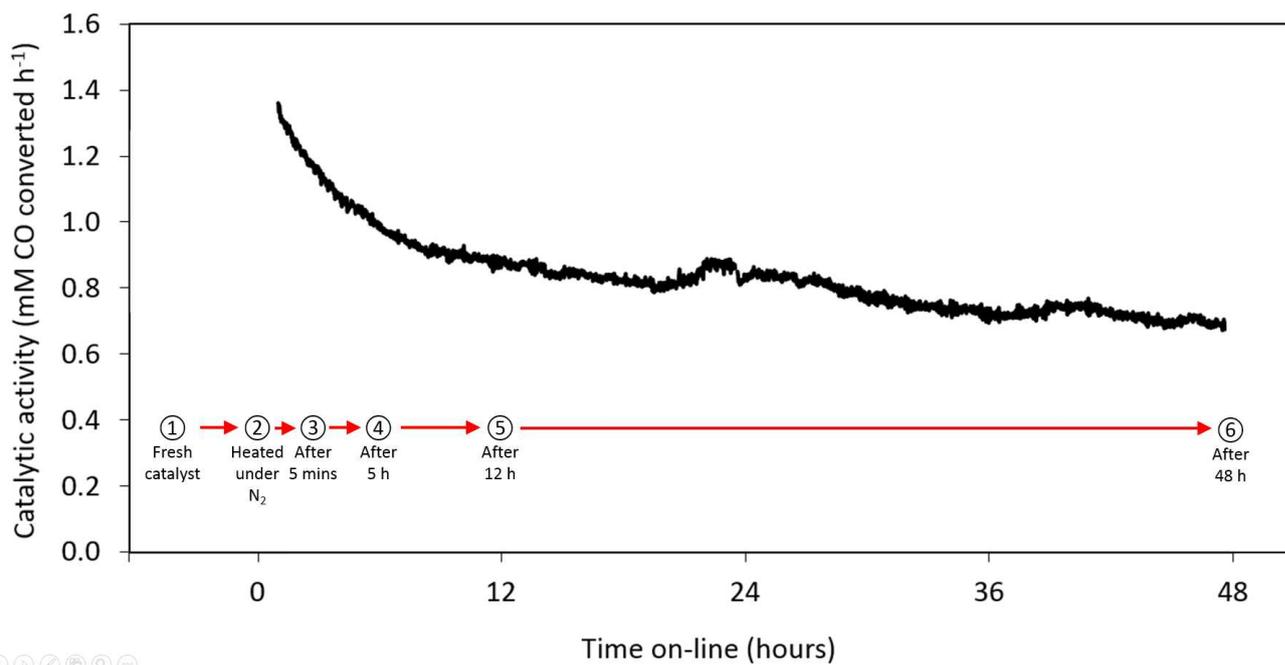| Sample	Oxidation state of Au species (%)		
	Au^0	Au^0*	Au^{3+}
Fresh ①	67.1	18.4	14.5
Heated under N_2 ②	77.9	15.0	7.1
5 h ④	85.0	15.1	0.0
48 h ⑥	88.5	11.6	0.0

Fig. 1. Time-on-stream profile of 2 wt% Au/CeZrO$_4$ under LTS conditions showing the intervals (①-⑥) at which the catalyst was characterised. 150 mg of catalyst was heated under N$_2$ to 150 °C at a ramp rate of 8 °C min^{-1} before switching to a feed of 2% CO, 2% CO$_2$, 7.5 % H$_2$O, 8.1% H$_2$ and 80.4% N$_2$. Total flow rate: 100 cm^3 min^{-1}; GHSV 52,000 h^{-1}.
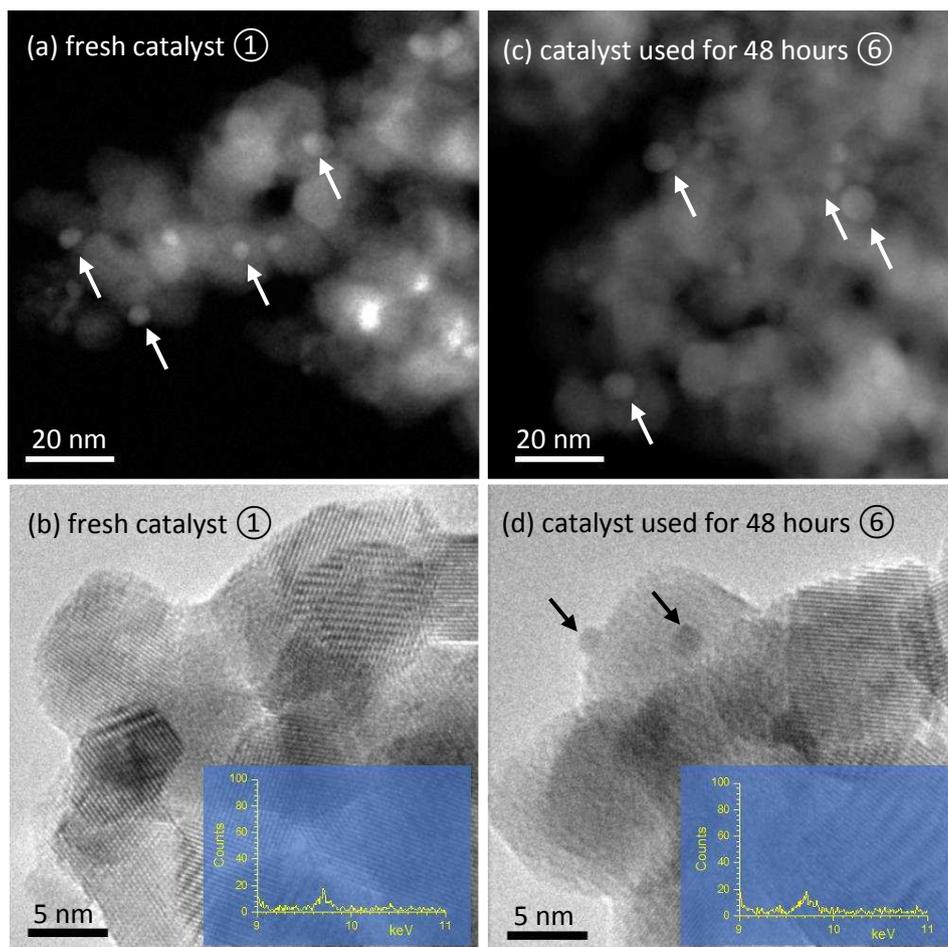
Fig. 2. Representative STEM-HAADF and TEM bright field images of the (a, b) fresh 2 wt% Au/CeZrO₄ catalyst ① and the same catalyst used under LTS conditions for 48 h ⑥. Similar Au particles about 10 nm in size are seen in both the fresh and used catalyst (white arrows in *(a)* and *(c)*). Smaller particles (< 2 nm) can be found in the used catalyst ⑥ (black arrows in *(d)*) but not in the fresh catalyst ①. XEDS analysis from the field of view in (b) and (d) showed a similar level of Au signal (image insets), strongly suggesting that the < 2 nm particles found in the used catalyst (black arrows in *(d)*) arise from the sintering/agglomeration of smaller Au species, which were not detected in the STEM images due to the high mass CeZrO₄ support material.
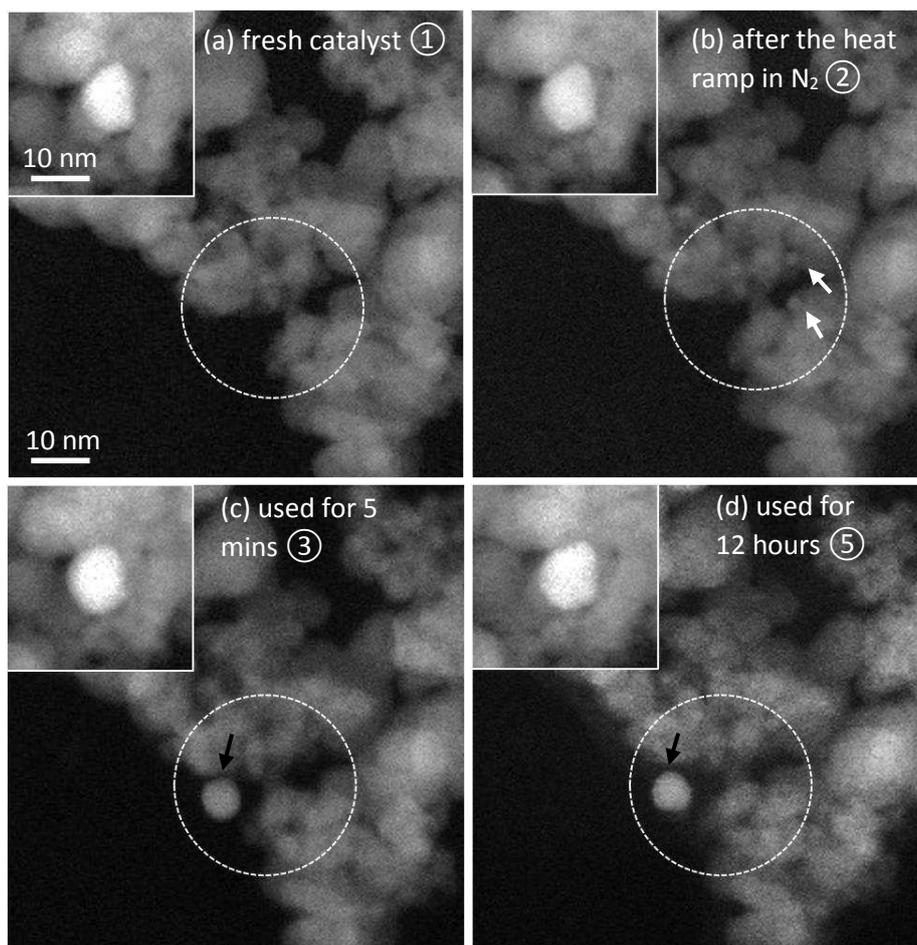
Fig. 3. Stop-start STEM HAADF images of the same region in a 2 wt% Au/CeZrO$_4$ catalyst at different stages of the LTS reaction: a) ① fresh catalyst; b) ② after the heat ramp under N$_2$; c) ③ after 5 mins on-stream and d) ⑤ after 12 h on-stream. As highlighted by the white dashed line circle in the fresh catalyst ①, only particles around 10 nm (inset) were seen, but no smaller particles were found. After the heat ramp in N$_2$, ② smaller Au particles <2 nm, shown by white arrows, were formed in the same area. At stage ③ those particles continued to sinter into larger particles (black arrow in *(c)*) and remained unchanged after an additional heat ramp plus 12 hours of reaction ⑤. The 10 nm particles that were present in the fresh catalyst remain largely unchanged throughout the process (image insets in *(a-d)*).
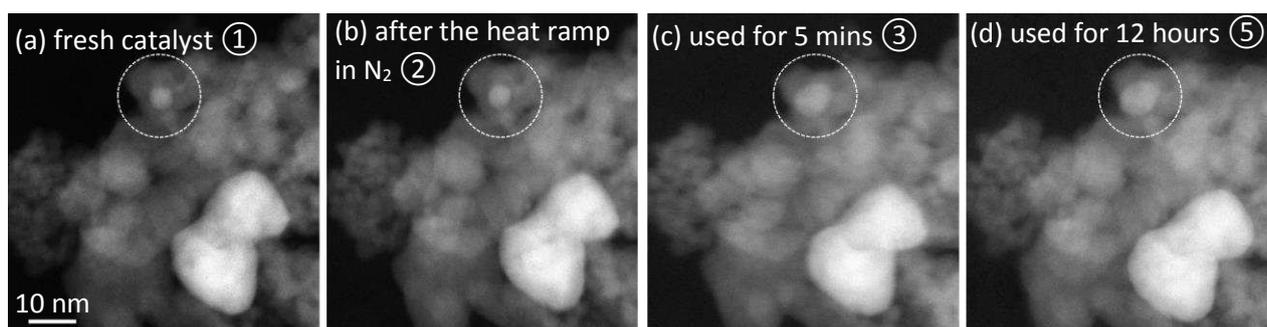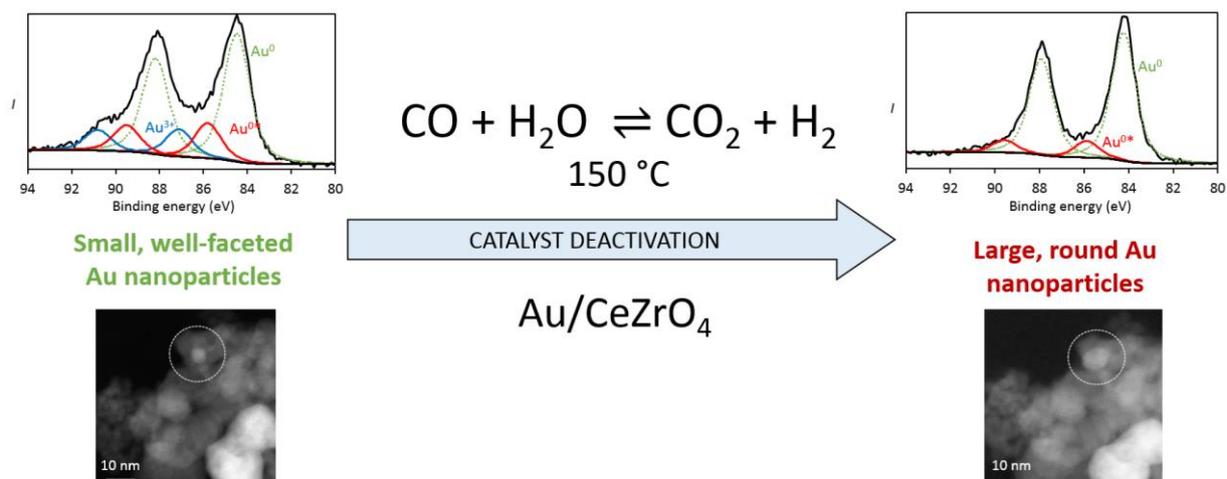
Fig. 4. An additional systematic set of stop-start STEM-HAADF images of the same area in a 2 wt% Au/CeZrO$_4$ catalyst at different stages of the LTS reaction. In this case, the highlighted Au particle that originally existed in the fresh catalyst shows significant growth from stage ② to stage ③ and ⑤.

Table of contents

$$CO + H_2O \rightleftharpoons CO_2 + H_2$$

150 °C

CATALYST DEACTIVATION

$Au/CeZrO_4$

Small, well-faceted Au nanoparticles

Large, round Au nanoparticles

Using stop-start STEM, the evolution of individual Au species was followed during the low-temperature water-gas shift reaction over $Au/CeZrO_4$. The formation of active Au nanoparticles during the heating of the catalyst to reaction temperature was observed, followed by further agglomeration of these species under reaction conditions. Complementary XPS also revealed that the deactivation of this catalyst proceeds through particle agglomeration.

Keywords: Gold, Nanoparticles, Water-gas shift, Deactivation, fuel cells